

# EFFECT OF NUCLEAR TRANSPARENCY FROM THE $(p,2p)$ MEASUREMENTS ON ${}^6\text{Li}$ AND ${}^{12}\text{C}$ AT 1 GeV.

V.N. Baturin, E.N. Komarov, V.V. Nelyubin,  
V.V. Sulimov and V.V. Vikhrov.

**St.-Petersburg Nuclear Physics Institute (PNPI),  
188350, Gatchina, Russia.**

July 31, 2021

## Abstract

We studied the production of protons to the backward direction in  $(p, 2p)$  reactions on  ${}^6\text{Li}$  and  ${}^{12}\text{C}$ , accompanied by a proton emitted into the forward hemisphere. The momenta of the final two protons were measured in a wide range with the two-arm time-of-flight spectrometer. For each event we reconstructed the mass of the intermediate off-shell particles. We observed that the  $\Delta(1232)$  is manifested in the mass spectra of intermediate baryons. A surprising angular dependence of the intermediate meson mass spectrum was revealed. Also we have discovered a strong narrow dip in the mass spectra of intermediate mesons at the mass of the real pion. We explain this effect as an abrupt decrease of the absorption probability for on-shell mesons (the pion-nuclear transparency).

*PACS:* 24.30Gd, 25.10+s, 25.75Ld

*Keywords:* NUCLEAR REACTIONS,  ${}^6\text{Li}$ ,  ${}^{12}\text{C}(p, 2p)X$ ,  $P=1.696\text{GeV}/c$ , isobar, cumulative protons, intermediate particle mass spectrum, correlation function, nuclear transparency.

## Introduction.

One of the exciting events in the study of proton-nucleus interactions at the energy scale of 1GeV has been the observation of a significant inclusive yield of energetic nucleons in the energy domain forbidden for free  $pN$  scattering (the cumulative effect)[1]. Further experiments revealed a universal exponential behavior of inclusive energy spectra for various projectiles and outgoing particles over a wide energy range (the so-called nuclear scaling)[2]. Since the momentum transfer can be very high in such processes, this universality suggests that the cumulative production of nucleons is relevant to the short-range properties of nuclear matter. An extensive theoretical analysis of the short-range phenomena in hadron- and lepton-nucleus interactions in the energy range from 0.6 to 400GeV has been given in ref.[3].

In this paper we report on the emission of a backward going cumulative proton ( $p_b$ ) accompanied by a forward going proton ( $p_f$ )

$$p + A \rightarrow p_b + p_f + X \quad (1)$$

on  ${}^6\text{Li}$  and  ${}^{12}\text{C}$  at a incident proton energy 1GeV. Our two arm time-of-flight spectrometer allowed the measurement of the energies and the directions of two final protons in coincidence. The experimental layout is shown in Fig.1. The details of the spectrometer and the measurements are described in Section 1.

From earlier investigations of the reaction (Eq.1) at 0.64, 0.8 and 1GeV we know that a significant part of the inclusive spectra can be related to phenomena concerning several elementary collisions, such as the mechanism of quasi-two-body scaling[4]-[7], proton scattering off a quasi deuteron pair[6, 7], scattering off short-range nucleon pairs[3], and to the isobar production in the intermediate state[8]. Hence, the dynamics of cumulative production appears complex. Nevertheless, we believe that there is a critical final collision in Eq.1, which results in the observable protons

$$x + t \rightarrow p_b + p_f, \quad (2)$$

where  $x$  is an intermediate off-shell particle, and  $t$  is a bound target nucleon (or nucleons). In our study we focus on two hypotheses, in which we assume that: (1)  $t$  is a bound nucleon, while  $x$  is an intermediate baryon (isobar) and (2)  $t$  is a bound nucleon pair, then  $x$  has to be an off-shell meson.

These hypotheses are referred to below as “isobar recombination” and “meson absorption” respectively (see Fig.1). Of course, the isobar may be produced at the pion-nucleon vertex. Therefore, we consider the meson absorption approach as providing a further insight into an earlier stage of the process, rather than an alternative to the isobar recombination.

Since the rest of the struck nucleus has not been detected in our experiment, the kinematics of the vertex Eq.2 is under-determined. Nevertheless, having measured the four-momenta of both protons, we can evaluate the invariant mass of the intermediate particle  $x$ , assuming  $t$  to be at rest:

$$m_x^2 = \mathbf{P}_x^2 = (\mathbf{P}_b + \mathbf{P}_f - \mathbf{P}_t)^2, \quad (3)$$

where  $\mathbf{P}_{b,f,t}$  are the four-momenta of final  $b$ - and  $f$ -protons and of the target nucleon(s) at rest. Actually,  $t$  is a bound object in motion, therefore  $m_x^2$  has to be modified by Fermi motion and by the rescattering of the protons in the final state. Using a simple estimate we show below that the bias has to be relatively small for the intermediate baryon. However, it may be significant for the process of intermediate meson absorption by a nucleon pair.

In the following Sections 2 and 3 we apply the method of correlation functions to study the reaction in Eq.1. First of all, we analyze our data in terms of model-independent kinematic variables, such as the energies of secondary particles. Next we investigate our first measured mass spectra of intermediate particles in both forementioned hypotheses and discuss the observed effects.

## 1 Experimental method.

The experiment was performed with the two-arm time-of-flight spectrometer [7]-[9], which was originally designed as a large acceptance neutron detector for investigation of (p,n) reactions[10]. Each arm of the spectrometer consists of a starting scintillator ( $10 \times 10 \times 0.5 \text{ cm}^3$ ) and a hodoscope of five large scintillators ( $20 \times 20 \times 100 \text{ cm}^3$ ), which form the “crystal wall” (CW) with the overall sensitive surface of  $1 \text{ m}^2$ . Each of the large crystals was viewed by photo-multipliers from both ends. The starting  $b$ - and  $f$ -counters were placed  $0.6 \text{ m}$  and  $1 \text{ m}$  apart from the target, and they spanned the area of corresponding CWs, placed  $7 \text{ m}$  and  $12 \text{ m}$  away from the target.

The external proton beam of the PNPI synchro-cyclotron entered the target ( $10 \times 10 \times 1 \text{ cm}^3$ ) placed in the focus of the spectrometer with a yaw minimizing the energy loss of secondary particles. The beam was monitored by a telescope of two scintillators, focused onto the thin foil window of the vacuum pipe upstream of the target.

In order to eliminate the propagation time of light in the long scintillators, the particle time of flight  $t_{i=b,f}$  has been evaluated as  $t_i = (t_{il} + t_{ir})/2$ , where  $t_{il(r)}$  are the time intervals between the signals from the start counters and from the left(right) photo-multipliers of the scintillator. Two samples of time-of-flight spectra are shown in the lower panel of Fig.2. The resolution in  $t_f$ , resulting from a set of test beam measurements, was about  $0.87 \text{ ns}$  (FWHM).

The velocities of secondary protons have been determined via the  $t_{b(f)}$  defined above, taking into account the energy losses along their trajectories. Since the coordinates of the interaction point in the target are unknown, the energy loss has been calculated assuming the event originated in the center of the target. This translates into an additional smearing of the particle energy. The resulting energy resolution in the energy range (100,250)MeV was between 9% and 4% for  $f$ -protons and between 10% and 8% for  $b$ -protons. At higher energies the resolution for  $f$ -protons decreased to 10% at 900MeV.

For the purpose of momenta reconstruction the coordinates of particle hits in both CWs have been measured. The vertical coordinate has been determined as the center of the hit scintillator in the hodoscope. The horizontal coordinate  $x$  has been measured by two independent methods. Firstly, the coordinate  $x_t$  has been measured via the light propagation time:  $2x_t = l_0 + c(t_{il} - t_{ir})$ , where  $l_0$  is the length of the scintillator,  $c$  is the speed of light in the scintillator. Secondly, in order to identify protons by energy loss, the signals from the starting counters and from both ends of the CWs have been integrated by ADCs. The ADC values have been used to measure the additional coordinate  $x_a$  in a following way. Due to attenuation of light in the counters, the charges  $q_{l(r)}$  measured at two ends of the scintillator relate to  $x_a$  as  $q_l = k_l(\Delta E)e^{-x_a/l_a}$  and  $q_r = k_r(\Delta E)e^{(x_a - l_0)/l_a}$ , where  $x_a$  is the coordinate to be measured,  $\Delta E$  is the original ionization,  $k_{l(r)}$  are the calibration constants, and  $l_a$  is the light attenuation length. Thus, both the total energy loss  $\Delta E$  and the coordinate  $x_a$  are known. A typical energy loss spectrum of backward going particles is shown in the top panel of Fig.2. The accuracy in the horizontal coordinate combined from the two methods  $x = (x_a + x_t)/2$ , measured with direct 1GeV proton beam, was about 7cm (FWHM). The

resolution in  $x$  for secondary particles was about 12cm (Fig.2).

The proton beam of the synchro-cyclotron of PNPI is delivered on a sequence of  $7ns$  long micro-bunches, separated by  $75ns$ . We have used this peculiarity of the beam timing for a crucial reduction of the background of accidental coincidences. The supplementary time interval  $t_{bf}$  between the hits in starting  $b$ - and  $f$ -counters has been digitized for every event. The interval between the birth times of  $b$ - and  $f$ -particles  $t_{bf}^*$  has then been reconstructed[11], using the obvious relation  $t_{bf}^* = t_{bf} - \tau_b + \tau_f$ , where  $t_{bf}$  is the measured time interval, and  $\tau_{b(f)}$  are the times of particle propagation between the target and the starting counters, evaluated via  $t_{b(f)}$  and the known distances. Since for real events the final particles emerge simultaneously, the value  $t_{bf}^*$  was found to be distributed around zero with standard deviation  $0.51ns$ , corresponding to the time resolution of the spectrometer. By contrast, the accidental events filled a significantly wider interval ( $14ns$ ) corresponding to the double width of the micro-bunch. We reduced the background of accidental events by an order of magnitude by implementing a cut on  $t_{bf}^*$ . This allowed us to take data at higher beam current with the same accidental background.

The total statistics of about  $10^5$  true coincidental events was accumulated during one week run. While taking data, the  $f$ -spectrometer has been successively positioned at  $\theta_f = 12.5^\circ$ ,  $25^\circ \pm 2^\circ$ ,  $39.5^\circ \pm 2.2^\circ$  and  $65^\circ \pm 2.5^\circ$ , while the  $b$ -spectrometer spanned the area  $\theta_b = -115^\circ \pm 4^\circ$  in the backward hemisphere.

## 2 Analysis.

We have analyzed our data using the method of correlation functions (c.f.'s) or, in other words, the reduced spectra[7, 8, 12, 13]. The substantial advantage of this technique is that c.f.'s, being the ratios of cross sections, are tolerant to relevant systematics, efficiencies, acceptance related effects and diverse cuts. The most remarkable benefit of this method is that, as we show below, the deviations of reduced spectra may contain a message from the final vertex. Thus, provided the final state and its phase space are unknown, this method allows us to access experimentally the dynamics of the process under study.

In terms of Probability one can consider the measured differential cross sections as a properly normalized probability density functions (p.d.f.'s). Let  $\mathbf{b} \in B$  and  $\mathbf{f} \in F$  be the random multicomponent kinematic variables of  $b$ - and

$f$ -protons. Here  $B$  and  $F$  are the corresponding manifolds of outcomes. For inclusive  $b$ - and  $f$ -events we introduce the p.d.fs of  $B$  as  $P_b(\mathbf{b}) \propto d\sigma^i/d\mathbf{b}$  and of  $F$  as  $P_f(\mathbf{f}) \propto d\sigma^i/d\mathbf{f}$ , both proportional to the inclusive differential cross sections. A coincidental event  $(\mathbf{b}, \mathbf{f})$  may be considered as an outcome from the manifold  $B \cap F$  with the joint p.d.f.  $P_{bf}(\mathbf{b}, \mathbf{f}) \propto d\sigma^c/d\mathbf{b}d\mathbf{f}$ , the double-differential cross section measured in coincidence. We involve in our analysis the combinatoric p.d.f.  $P_{bf}^c(\mathbf{b}, \mathbf{f}) = P_b(\mathbf{b})P_f(\mathbf{f})$ , which has been measured using pairs of recorded inclusive  $b$ - and  $f$ -events. We also use the conditional p.d.f.  $Q(\mathbf{b}|\mathbf{f}) = P_{bf}(\mathbf{b}, \mathbf{f})/P_f(\mathbf{f})$ , evaluated at given  $\mathbf{f}$ .

First of all, we present our data in terms of the single particle correlation function  $S_f$  given by<sup>1</sup>

$$S_f(\mathbf{b}) = \frac{Q(\mathbf{b}|\mathbf{f})}{P_b(\mathbf{b})} \propto \frac{d\sigma^c/d\mathbf{b}d\mathbf{f}}{d\sigma^i/d\mathbf{b}}. \quad (4)$$

From the definition of conditional probability one immediately obtains

$$\frac{Q(\mathbf{b}|\mathbf{f})}{P_b(\mathbf{b})} = \frac{P_{bf}(\mathbf{b}, \mathbf{f})}{P_b(\mathbf{b})P_f(\mathbf{f})}. \quad (5)$$

Two random variables are independent if and only if  $P_{bf}(\mathbf{b}, \mathbf{f}) = P_b(\mathbf{b})P_f(\mathbf{f}) = P_{bf}^c(\mathbf{b}, \mathbf{f})$ . Hence, due to Eqs. 4,5 the c.f.  $S_f$  must be unity, that is  $Q(\mathbf{b}|\mathbf{f}) = P_b(\mathbf{b})$  for independent emission of  $b$ - and  $f$ -protons. The last relation may be integrated over any number<sup>2</sup> of components of  $\mathbf{b}$  and  $\mathbf{f}$ . Applied to the measured spectra, this leads to an important statement: for independent emission of particles

$$S_f(b) \propto \frac{(d\sigma^c/db)_f}{(d\sigma^i/db)} = \text{const}(b), \quad (6)$$

where  $b$  is a scalar variable related to the  $b$ -proton, such as the kinetic energy. The index  $f$  means that the cross section is integrated over  $\mathbf{f} \in f \subset F$ . Thus, if the measured c.f.  $S_f(b)$  deviates from a constant<sup>3</sup>, then, very likely, a signal from a common vertex of  $b$ - and  $f$ -protons is being observed.

<sup>1</sup>Similarly, we define  $S_b$  with all the following formulas valid at  $\mathbf{b} \rightleftharpoons \mathbf{f}$ .

<sup>2</sup>In the following formula we integrate it over all but one components of  $b$ .

<sup>3</sup>Absolute normalization of  $S$  is not important.

A particularly promising way of studying the process Eq.1 is by means of the mass spectra of intermediate particles. Let us consider the c.f. constructed from the inclusive and double differential cross sections:

$$R(\mathbf{v}) = \frac{P_{bf}(\mathbf{v})}{P_{bf}^c(\mathbf{v})} \propto \frac{d\sigma^c/d\mathbf{b}d\mathbf{f}}{(d\sigma^i/d\mathbf{b})(d\sigma^i/d\mathbf{f})}, \quad (7)$$

where  $P_{bf}$  and  $P_{bf}^c$  are the coincidental and combinatoric p.d.f's introduced above. We consider them to be functions of the compound vector  $\mathbf{v} = (\mathbf{b}, \mathbf{f})$ . The ratio of density functions  $R(\mathbf{v})$  can be expressed via a new variable  $\mathbf{u} = \mathbf{u}(\mathbf{v})$ , using the technique of Jacobians, which obviously are canceled in the ratio. If the final protons emerge independently, then again  $P_{bf}(\mathbf{u}) = P_{bf}^c(\mathbf{u})$ . One may integrate this relation over any components of  $\mathbf{u}$ , and we obtain<sup>4</sup> another useful statement, valid for independent emission

$$R(u_i) = \frac{P_{bf}(u_i)}{P_{bf}^c(u_i)} = 1 \propto \text{const}(u_i), \quad (8)$$

where  $P_{bf}(u_i) = \int \prod_{j \neq i} du_j P_{bf}^c(\mathbf{u})$  and  $u_i$  is a scalar variable, such as invariant mass of an intermediate particle. Thus, a deviation of the measured two particle c.f.  $R(m_x)$  from a constant<sup>5</sup> may be considered as an indicative of an intermediate particle  $x$ .

### 3 Results and discussion.

The inclusive energy spectra of  $b$ - and  $f$ -protons, used for evaluation of c.f.'s, are shown in Fig.3. First we focus on c.f.  $S_f$ , measured at  $\theta_f=65^\circ$  and shown in Fig.4 as a function of kinetic energy of  $b$ -protons ( $T_b$ ). In this figure  $S_f(T_b)$  scales in units of differential multiplicity, i.e. having multiplied  $S_f$  by the solid angle of the  $f$ -spectrometer, one obtains the mean number of  $f$ -protons accompanying the single  $b$ -proton of energy  $T_b$ .

Noticeable deviations from a constant are seen in the vicinity of 100 MeV on both targets. The relative amplitude of the deviation is obviously  $A$ -dependent. The shape of  $S_f$  varies with the energy of the  $f$ -proton. To further investigate these deviations, the reduced energy spectra of both  $b$ -

<sup>4</sup>Integrating over all, but one components of  $\mathbf{u}$ .

<sup>5</sup>We do not normalize the measured  $R$  to unity since the normalization is not important.

and  $f$ -protons have been studied for their dependence on the energy of the partner. The example of such a “cross-reference” study at  $\theta_f=25^\circ$  is shown in Fig.5. A narrow peak shows up at  $115\pm 4\text{MeV}$  in the shape of  $S_f(T_b)$  when the energy of  $f$ -proton increases<sup>6</sup>. The amplitude of this peak reaches a maximum at  $f$ -proton energy in the interval  $(210, 270)\text{MeV}$ . The deviation is also evident in  $S_b(T_f)$  as a bump at  $f$ -proton energy  $237 \pm 10\text{MeV}$ . Both fitted “characteristic” energies are in agreement with the kinematics of the two-stage intra-nuclear process  $pp_1 \rightarrow \Delta^+p$ ,  $\Delta^+p_2 \rightarrow p_b p_f$  involving the slow<sup>7</sup> isobar and the protons ( $p_{1,2}$ ) from the nucleus[8]. We note that the sum of characteristic energies (352MeV) corresponds to a kinetic energy of the isobar of 58MeV. If scaled to the beam energy, this value agrees with the measured spectrum of isobars from  $pp \rightarrow \Delta^+p$  at 1.47GeV[14] which has a maximum corresponding to an isobar energy of 80MeV.

The cross reference study had been also performed at  $\theta_f = 39.5^\circ$  and  $65^\circ$ , and similar indications of the isobar recombination process were observed[8]. We find it fascinating that the isobar recombination mechanism is manifest even in the reduced spectra of model independent variables.

Other very interesting observations can be made on the mass spectra of intermediate particles[7, 8]. An example of the initial intermediate baryon mass spectrum is shown in Fig.6 in comparison with the corresponding combinatoric spectrum. The two-particle correlation function  $R$  v.s.  $m_x$  (the intermediate baryon mass) is shown in Fig.7 at three angles of the forward-going proton.

A strong deviation of  $R(m_x)$  is distinctly seen in Fig.7 at  $\theta_f=39.5^\circ$  and  $65^\circ$  as a peak in the vicinity of the  $\Delta(1232)$  resonance. The centroids ( $1173\pm 3$ ,  $1156\pm 3\text{MeV}$ ) and the widths ( $150\pm 10$ ,  $130\pm 10\text{MeV}$ ) obtained in a fit are close to the parameters of the isobar. The isobar peak is quite prominent at  $39.5^\circ$  and  $65^\circ$ , but at  $25^\circ$  it is hidden by the events of the quasi two-body scattering[7], which are spread between 1.2 and 1.6GeV. Nevertheless, some indications of the isobar at  $25^\circ$  have already been shown in Fig.5.

From the behavior of both  $R$  and  $S$  we have estimated the  $\theta_f$ -dependence of the  $\Delta$  recombination yield, which is plotted in Fig.8. Integrating this curve over  $\theta_f$  and the azimuth<sup>8</sup>, we have roughly estimated the total yield of

---

<sup>6</sup>The numbers are from a fit by the sum of a Gaussian and polynomials.

<sup>7</sup>The “slow” (“fast”) isobar may be produced on the target(projectile) nucleons.

<sup>8</sup>We assume the azimuthal distribution to be uniform.



$\Delta$ -recombination process to be about 20% of the inclusive yield at  $115^\circ$ .

There are several experimental indications that nuclear medium effects do modify the parameters of the  $\Delta$  resonance[15]. With this concern we notice that the centroids of the isobar peak at  $39.5^\circ$  and  $65^\circ$  (Fig.7) are displaced to lower mass by  $59\pm 3$  and  $76\pm 3$ MeV respectively.

To estimate the influence of Fermi motion on the position of the isobar peak on the mass scale one may compare the yield of Eq.3 at  $\mathbf{P}_t = (m_t, \vec{0})$  with the value  $m_x'^2$ , calculated for an off-shell object  $t$  in motion, i.e. at  $\mathbf{P}_t = \mathbf{P}'_t = (E_t, \vec{p}_t)$ . In every event the difference of these values is given by

$$m_x^2 - m_x'^2 = (\mathbf{P}'_t - \mathbf{P}_t)(2(\mathbf{P}_b + \mathbf{P}_f) - (\mathbf{P}'_t + \mathbf{P}_t)) = 2(E_t - m_t)(E_b + E_f) - 2(\vec{p}_t, \vec{p}_b + \vec{p}_f) - E_t^2 + \vec{p}_t^2 + m_t^2. \quad (9)$$

Considering Eq.9 as the operator on vector  $|t\rangle$ , one obtains the eigenvalue of  $\hat{m}_x'^2$  in the form

$$\langle \hat{m}_x'^2 \rangle - m_x^2 = -2\varepsilon_t(E_b + E_f - m_t) - \langle \hat{p}_t^2 \rangle + \varepsilon_t^2, \quad (10)$$

where  $\varepsilon_t = \langle \hat{E}_t \rangle - m_t$  is the binding energy. We estimate the value of  $\langle \hat{p}_{t=N}^2 \rangle$  via the wave functions<sup>9</sup> of  ${}^6Li$  given in ref.[16], and we find from Eq.10, at “characteristic” values of  $E_b$  and  $E_f$ , that Fermi motion on  $P$ - and  $S$ -shells may shift the mass by  $-5.5 \pm 0.3$ MeV and by  $17 \pm 1$ MeV, respectively<sup>10</sup>. Hence, the contribution from Fermi motion can not be entirely responsible for the observed displacement.

The mass spectrum of intermediate particles may be affected by the rescattering of outgoing protons. An approach similar to Eq.9, applied to elastic rescattering of protons, yields[7]

$$m_x'^2 - m_x^2 = -2p_b p_f \sin^2 \phi (-\cos(\theta_b + \theta_f) + (2m_N)^{-2} p_b p_f), \quad (11)$$

where  $p_{b,f}$  are the momenta of protons and  $\phi$  is the rescattering angle in the laboratory system. Thus the contributions from both Fermi motion and from rescattering (at  $\bar{\phi} \approx 0.5$ ) in principle may be the cause of the observed displacement of the isobar peak. Another option, not investigated yet, may relate to the  $P_{33}$  nature of the isobar. The point is that, perhaps, isobar

<sup>9</sup> $|1P_{3/2}\rangle$ :  $\varepsilon_N = -5.8$ MeV,  $\langle \hat{p}_N^2 \rangle = .028$ GeV<sup>2</sup>.  $|1S_{1/2}\rangle$ :  $\varepsilon_N = -23$ MeV,  $\langle \hat{p}_N^2 \rangle = .017$ GeV<sup>2</sup>.

<sup>10</sup>The error bars here account for the width of the isobar.

formation may be enhanced for slow  $S$ -wave pions due to their interaction with  $P$ -shell nucleons carrying the desired angular momentum.

It should be emphasized that unlike the case of isobar recombination process, the effects of Fermi motion and rescattering may be essential for the meson absorption mechanism. Within this approach  $t$  is an  $NN$ -pair, and Eq.10 takes the form

$$\langle m_x'^2 \rangle - m_x^2 = 2 | \varepsilon_{NN} | (T_b + T_f) - \langle \hat{p}_{NN}^2 \rangle + \varepsilon_{NN}^2. \quad (12)$$

Assuming that the target nucleons are uncorrelated, we estimate  $\langle \hat{p}_{NN}^2 \rangle \approx 2\langle \hat{p}_N^2 \rangle$  and  $\varepsilon_{NN} \approx 2\varepsilon_N$ . Due to the negative term  $-\langle \hat{p}_{NN}^2 \rangle$ , Eq.12 yields  $(-4.9 \pm 0.14)10^{-2}\text{GeV}^2$  and  $(0.1 \pm 0.57)10^{-2}\text{GeV}^2$  for  $P$ - and  $S$ -shells respectively. Hence, for the reasons mentioned above, one may expect that the major fraction of the measured events<sup>11</sup> would display a negative  $m_x^2$ .

However, the data analyzed in the framework of the meson absorption hypothesis shows a very surprising behavior. The  $\theta_f$  dependence of the yield corresponding to  $m_x^2 > 0$  is shown in Fig.8 by the open squares. It follows the angular dependence of the isobar recombination yield (filled circles). At the same time, the fractional yield, measured as the ratio of positive  $m_x^2$  yield to the total yield (filled squares), rises rapidly from 5% to 92% (open circles). The latter value is quite surprising since, contrary to our expectation from Eq.12, most of the events do exhibit positive  $m_x^2$ .

As for the events with negative  $m_x^2$ , we note that in principle the squared four-momentum of the virtual meson, mediating the quasi-free process  $p + (pn) \rightarrow p_b + p_f + n$  on  $pn$ -pair, has to be negative. The point is that in such a process the virtual meson is emitted by the projectile proton. Therefore the squared mass of intermediate meson may be evaluated as  $m_x^2 = (P - P_n)^2$ , where  $P$  and  $P_n$  are the four-momenta of the initial proton ( $p$ ) and of the scattered neutron ( $n$ ) after emission of a virtual pion. The resulting value is obviously negative since  $(P - P_n)^2 = -2m_p T_n$ , where  $T_n$  is the kinetic energy of the final neutron in the rest frame of the projectile. Hence, the high relative yield of events with  $m_x^2 < 0$  at low  $\theta_f$  may be explained by dominance of the process of proton scattering off nucleon pairs, which is an essential feature of the model[3]. The observed sharp build up of the positive  $m_x^2$  yield at higher  $\theta_f$  implies, apparently, that in these events, prior to ultimate absorption, the meson has its momentum changed via interactions with other target nucleons.

---

<sup>11</sup>Unless only  $S$ -shell nucleons are involved in the process.

We now consider more closely the events with positive  $m_x^2$ . For such events the spectra of reduced mass of the intermediate meson have been investigated within the meson absorption hypothesis. The samples of original mass spectra are shown in Fig.9 together with the combinatoric spectra. The resulting reduced spectra from  ${}^6\text{Li}$  at three emission angles of  $f$ -protons are plotted in Fig.10.  $R(m_x)$  at  $25^\circ$  is nearly constant, while strong deviations are seen at  $39^\circ$  and  $65^\circ$ .

The reduced mass spectrum at  $\theta_f=65^\circ$  is very interesting. This spectrum exhibits an obvious dip in the vicinity of the pion mass. In order to measure the width and location of this dip it is natural to fit this spectrum by a sum of polynomials minus a Gaussian. The fitted centroid of the dip thus obtained,  $138 \pm 2\text{MeV}$ , agrees nicely with the mass of pion, while its standard deviation ( $30 \pm 3\text{MeV}$ ) is close to the mass resolution of the spectrometer, pointing out that the real width of the dip may be significantly smaller. To ensure this observation, we have investigated the reduced mass spectrum from  ${}^{12}\text{C}$  in comparison with the  ${}^6\text{Li}$  data (Fig.11). The same narrow dip at  $135 \pm 2\text{MeV}$  is evident in the  ${}^{12}\text{C}$  spectrum. It is worth mentioning that the amplitude of the deviation divided by  $R(0)$  scales as  $A^{-1}$  within  $\pm 7\%$  accuracy, and we find it encouraging to see a noticeable  $\theta_f$ - and  $A$ -dependence of the spectrum shape. So this effect is obviously not an instrumental artifact.

We can suggest the following, perhaps naive interpretation of this previously unknown effect. In the framework of the meson absorption hypothesis we probe the mass of the intermediate off-shell meson ( $m_x$ ) in a wide range. As  $m_x$  approaches the mass of real pion from either side, the probability of absorption from the intermediate state drops. It may well be that such behavior reflects the obvious fact that a real meson has a chance to escape from the nucleus into the free space, rather than to be absorbed by nucleons, while the virtual meson has not other options but to be absorbed inside the nucleus. Hence, a narrow dip at the mass of pion builds up, as if the nuclear medium is more "transparent" for real mesons.

It is evident from the large relative yield of positive  $m_x^2$  as well as from the dip location, which matches perfectly to the pion mass, that neither Fermi motion nor rescattering influence this effect. We emphasize that it is the term  $-\langle \hat{p}_{NN}^2 \rangle$  in Eq.12 that may change  $m_x^2$  to negative values, and, in contrast with the case of a single nucleon target, this term can be even zero for a nucleon pair if, for example, the couple populates the same nuclear shell with opposite momenta. Since the typical momentum transfer in the

process of virtual pion absorption exceeds  $0.5fm^{-1}$ , such a pair could be a short-range  $np$ -correlation[3], which apparently has been observed recently in  $^{12}C(p, 2p + n)$  measurements[17].

## 4 Conclusion.

The mechanism of production of cumulative protons on light nuclei was studied implementing the method of correlation functions. Evidence for the isobar recombination mechanism were found in the reduced spectra of kinetic energies of secondary protons. A more profound study was performed by measuring the reduced spectra of the intermediate baryon mass. These spectra were found to contain a pronounced peak in the region of  $\Delta(1232)$ .

In order to investigate further the earlier stages of the process, the same statistics were analyzed as the process of intermediate meson absorption by a nucleon pair. Two surprising phenomena were revealed within this approach.

The first is that the fractional yield of events with positive  $m_x^2$  builds up rapidly with the angle between the two final protons.

The second interesting phenomenon is the narrow dip in the reduced mass spectra of intermediate off-shell mesons, positioned at the mass of real pion. The concept of pion-nuclear transparency has been suggested for interpretation of this phenomenon.

In principle, the effect of pion-nuclear transparency may show up in collisions of heavy ions at high energy. If this effect reflects the nuclear shell structure, then the condition must hold that the shell structure remains unbroken. Nuclear shells may be destroyed in any transition of nuclear matter into a new state, such as the quark-gluon plasma, and, perhaps, such a transition could be indicated via this phenomena. We therefore appeal for further experimental and theoretical studies of this interesting effect. In particular, it would be very productive to investigate the  $A$ - and  $\theta_f$ -dependencies of the transparency dip with improved momentum resolution.

We are indebted to the PNPI synchro-cyclotron crew for the excellent proton beam. We acknowledge L.L.Frankfurt, M.I.Strikman and M.B.Zhalov for useful discussions and valuable comments on a draft of this paper.

The preliminary results have been published in [7, 8, 9].

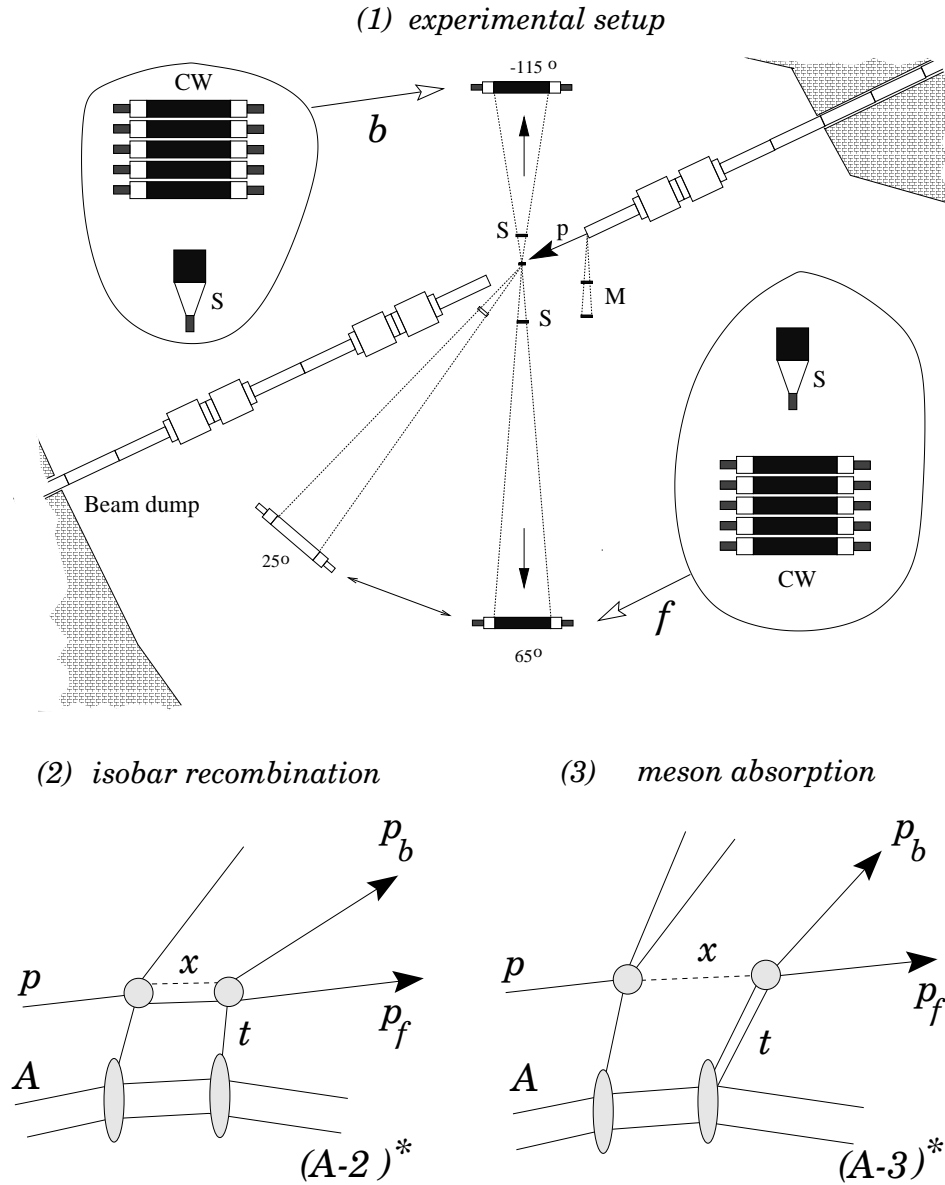


Figure 1: (1) Experimental layout: "p" - the proton beam, "M"- monitoring telescope, "S"-starting counters, "b"-backward Crystal Wall(CW), "f"-forward CW. The inserts show the front view of CWs and the starting counters. (2)The process of isobar ( $x$ ) recombination on a nucleon ( $t$ ). (3)The process of meson ( $x$ ) absorption by a nucleon pair ( $t$ ).

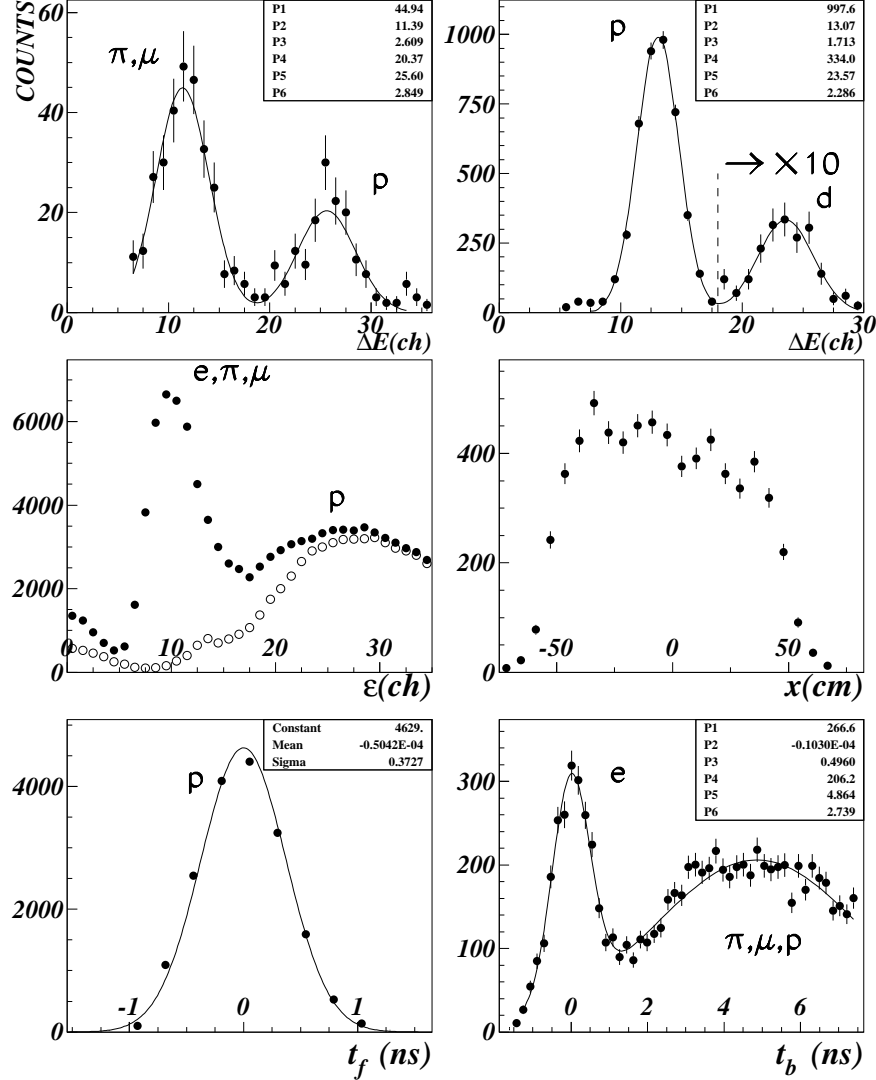


Figure 2: Distributions relevant to the spectrometer performance. The panels in this figure are referred to below as “row-column”. (1-1)The sample of energy loss ( $\Delta E$ ) spectrum for backward going particles at the velocity corresponding to  $210 \pm 10$  MeV protons. (1-2)The same at the proton energy of  $75 \pm 5$  MeV. (2-1)Energy loss ( $\varepsilon$ ) in the starting  $b$ -counter. Open circles show the spectrum of particles selected at  $\Delta E$  typical for protons. (2-2)Distribution of the  $x$ -coordinate of backward going particles. (3-1)TOF spectrum of 1 GeV beam protons. FWHM is  $0.87 ns$ . (3-2)TOF spectrum of backward going particles at 6.5m apart the target. FWHM of the electron peak is about  $1.2 ns$ .

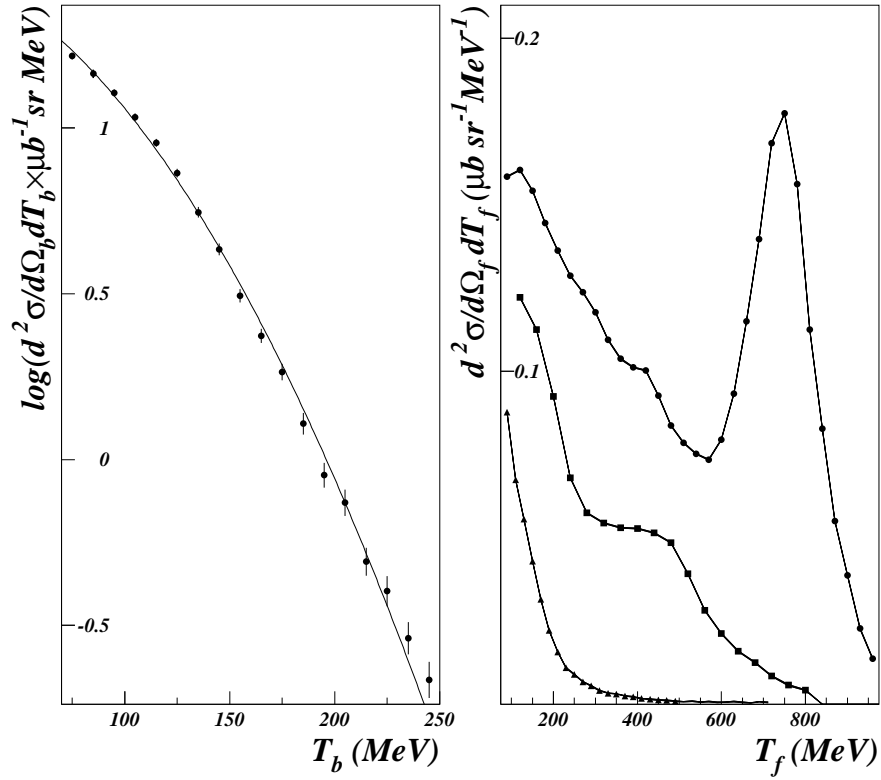


Figure 3: Kinetic energy spectra of inclusive  $b$ - and  $f$ -protons from the  ${}^6Li$  target. Left:  $T_b$  spectrum at  $115^\circ$ . Right: (1)circles -  $T_f$  spectrum at  $\theta_f=25^\circ$ . Peak at 745MeV(sigma 69MeV) corresponds to quasi-elastic  $pN$ -scattering. (2)squares - at  $39.5^\circ$ . The quasi-elastic peak is evident at  $470 \pm 10$ MeV (sigma 79MeV). (3)triangles - at  $65^\circ$ . Solid lines are shown to guide the eye.

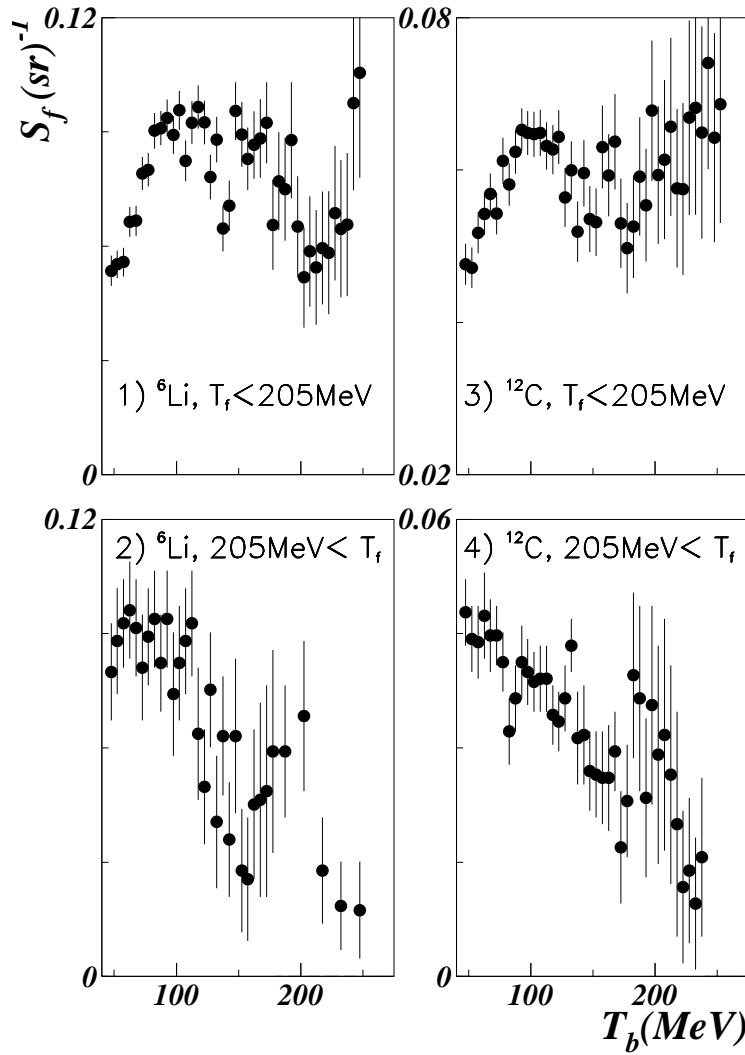


Figure 4: Correlation function  $S_f$  for target  ${}^6Li$  at  $\theta_f = 65^\circ$  vs  $T_b$ , the kinetic energy of backward going proton: (1) at  $T_f \leq 205 MeV$  and (2) at  $T_f > 205 MeV$ . The same for target  ${}^{12}C$ : (3) at  $T_f \leq 205 MeV$  and (4) at  $T_f > 205 MeV$ .



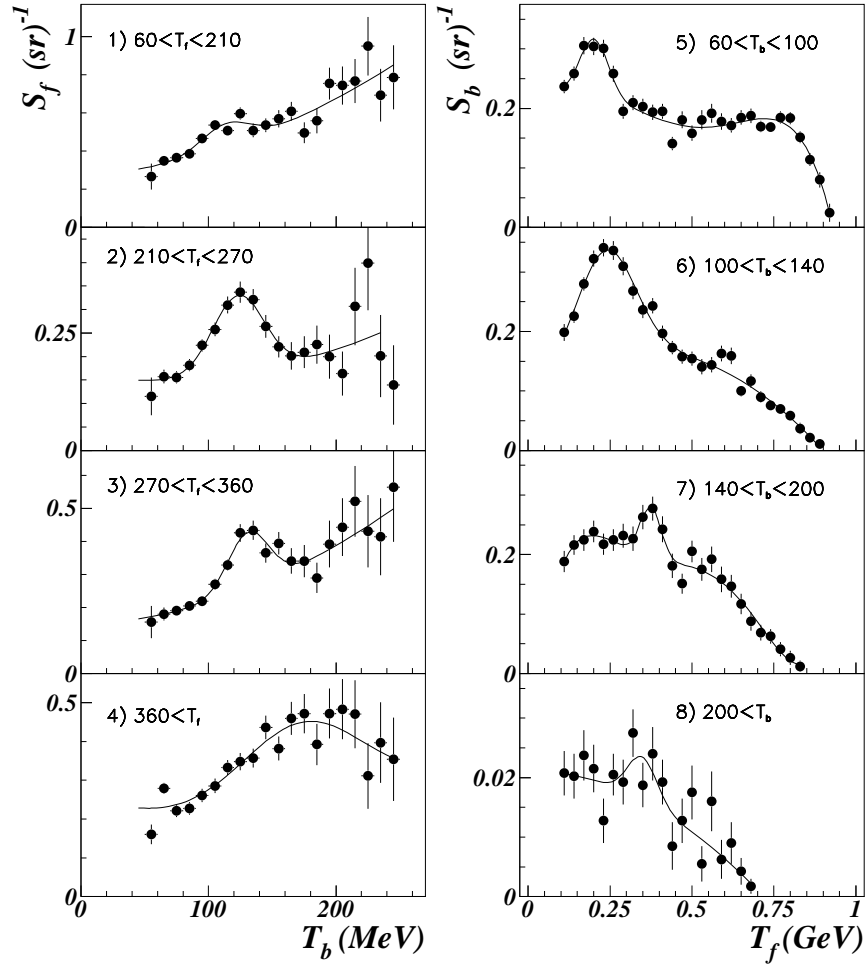


Figure 5: Cross reference study of  $S_b$  and  $S_f$  for  ${}^6\text{Li}$  at  $\theta_f=25^\circ$ . (1-4)  $S_f(T_b)$  for different intervals of  $T_f$  specified in each fragment. (5-8)  $S_b(T_f)$  for different intervals of  $T_b$ . Solid curves are the fits by a Gaussian plus polynomials.

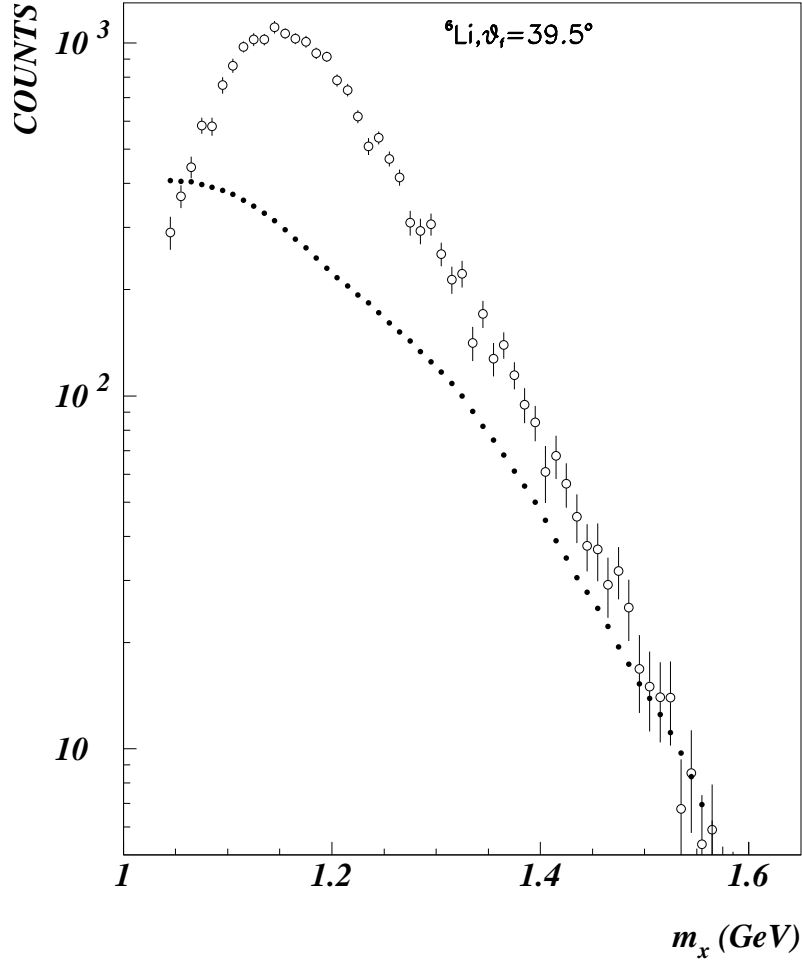


Figure 6: The spectra of intermediate baryon mass( $m_x$ ) from  ${}^6\text{Li}$  at  $\theta_f=39.5^\circ$ . The mass is calculated within the  $\Delta$  recombination hypothesis. The open circles show the raw mass spectrum. The black points represent the combinatoric spectrum with an arbitrary normalization. The statistical errors are less than the symbol size.

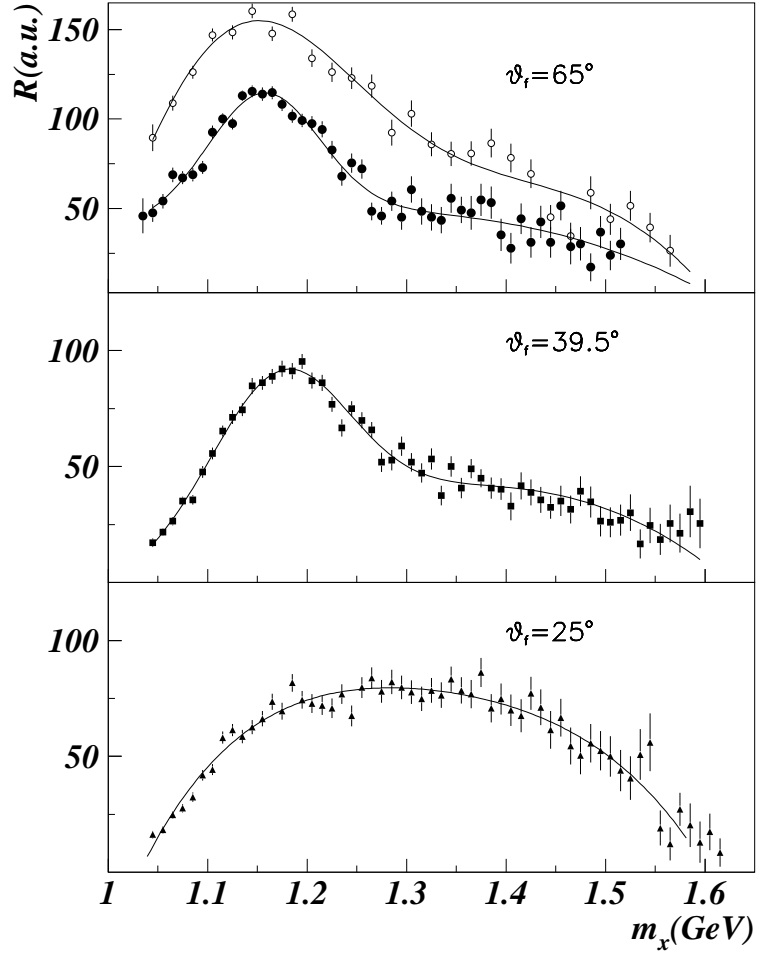


Figure 7: Correlation function  $R$  on targets  ${}^6\text{Li}$  (filled symbols) and  ${}^{12}\text{C}$  (open circles) vs  $m_x$ , the mass of intermediate baryon, calculated within the isobar recombination hypothesis at  $\theta_f$ : (1)  $65^\circ$  (circles), (2)  $39.5^\circ$  (squares), (3)  $25^\circ$  (triangles). Solid curves are the fits by a Gaussian plus polynomials.

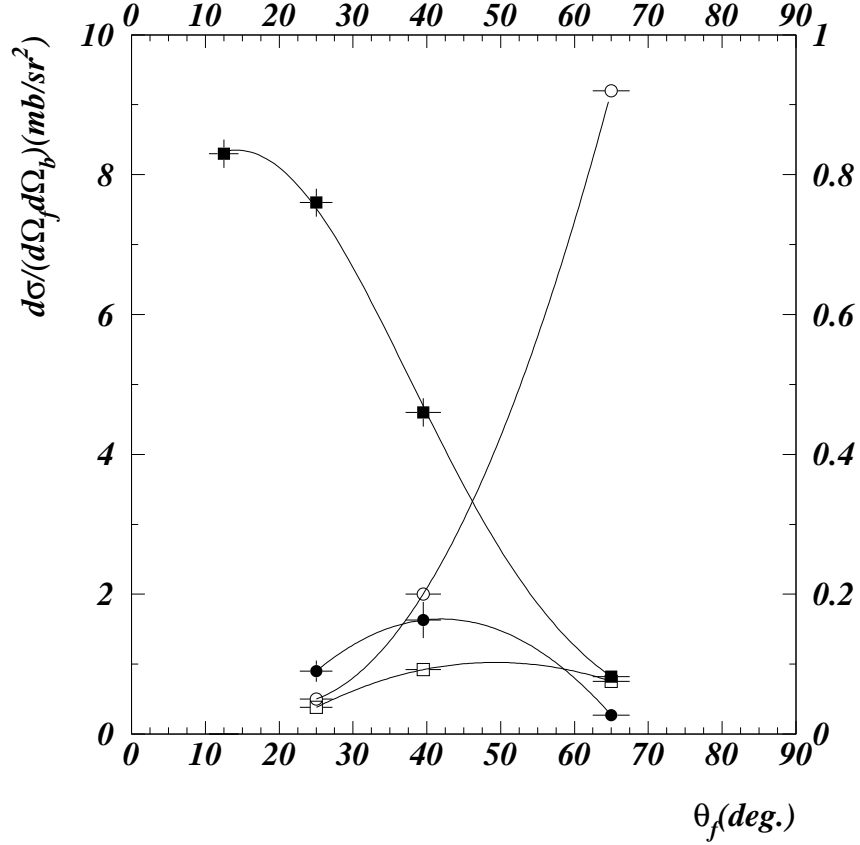


Figure 8: Cross sections vs the angle of the forward-going proton( $\theta_f$ ). (1) The total yield of the coincident  $b$ - and  $f$ -protons (filled squares). (2) The yield from the  $\Delta$  recombination process (filled circles). (3) The yield of positive  $m_x^2$  within the meson absorption hypothesis (open squares). (4) The ratio of the positive  $m_x^2$  yield to the total yield (open circles, right scale). Shown by solid curves are the fits by polynomials to guide the eye.

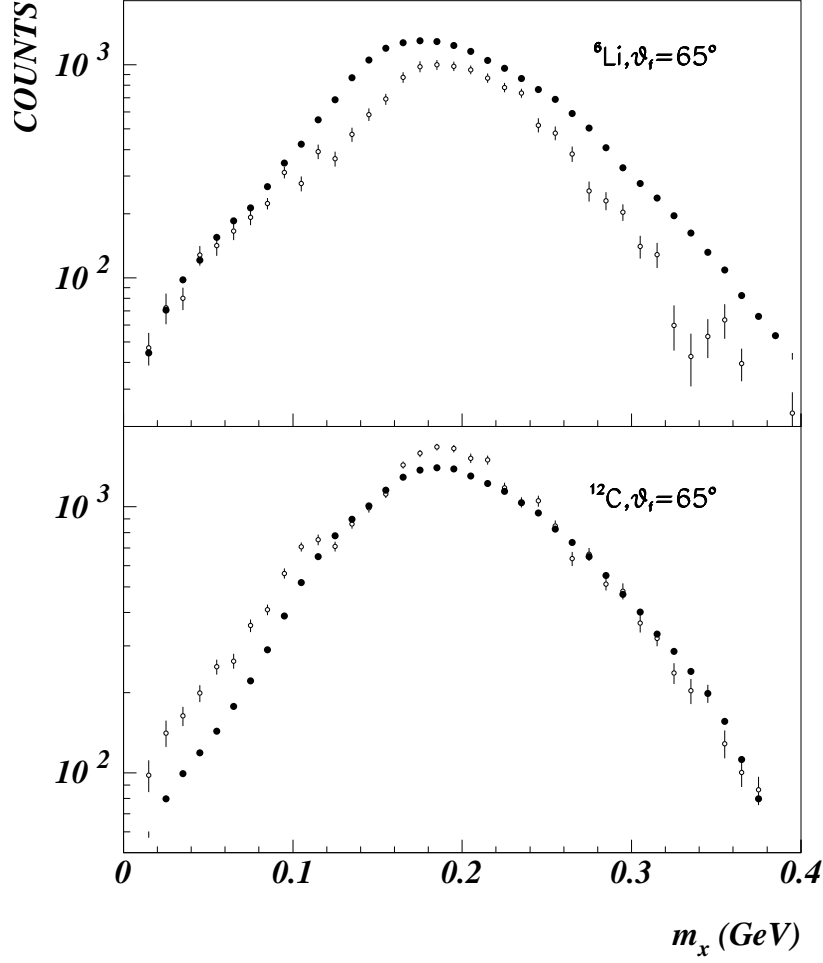


Figure 9: The mass spectra of intermediate pions at  $\theta_f = 65^\circ$  from  ${}^6\text{Li}$  (top panel) and  ${}^{12}\text{C}$  (bottom panel) targets. Open circles are the raw mass spectra evaluated from the momenta of  $b$ - and  $f$ -protons. The black dots represent the combinatoric spectra evaluated from the pairs of inclusive  $b$ - and  $f$ -protons. Normalization of the combinatoric spectra is arbitrary. The statistical errors are less than the symbol size.

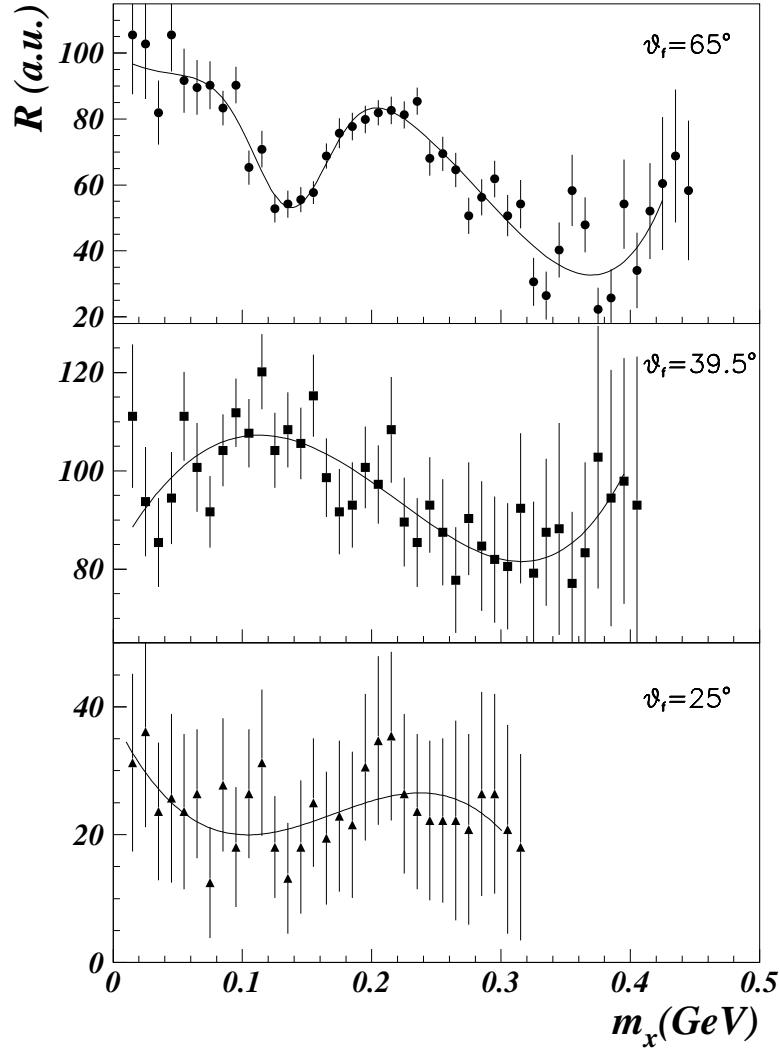


Figure 10: Correlation function  $R$  on  ${}^6\text{Li}$  vs the mass of virtual meson ( $m_x$ ), calculated within the meson absorption hypothesis at  $\theta_f =$  (1) $65^\circ$ (circles), (2) $39.5^\circ$ (squares) and (3) $25^\circ$ (triangles; the last 15 points are smoothed). Solid curves are the fits by a Gaussian plus polynomials.

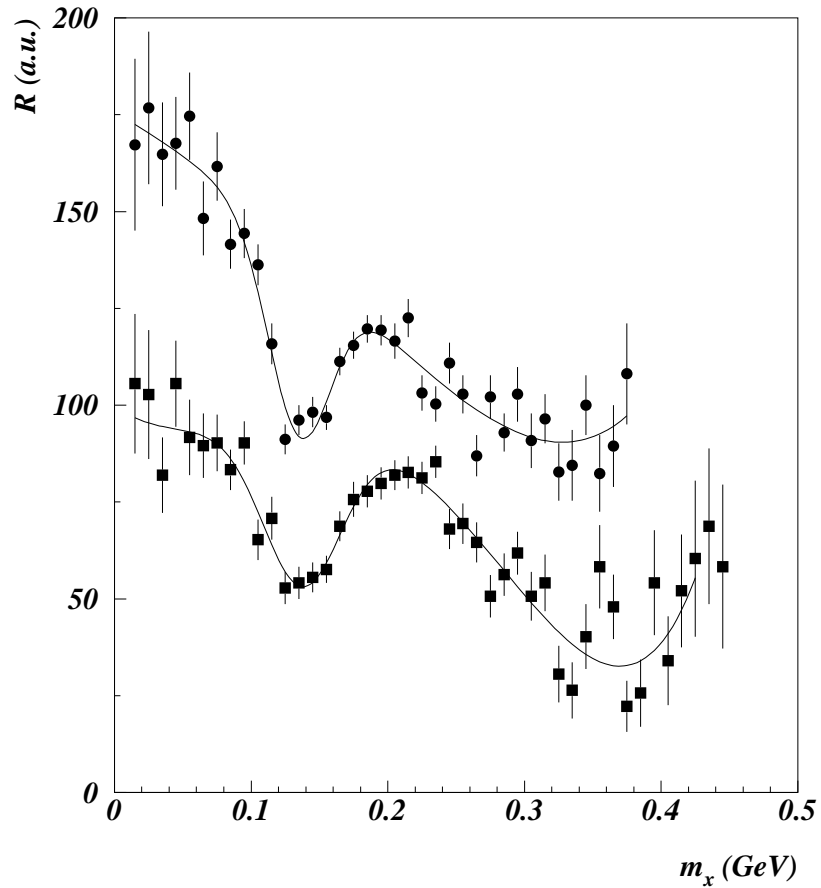


Figure 11: The nuclear transparency effect. The correlation function  $R$  at  $\theta_f = 65^\circ$  on targets  $^{12}\text{C}$ (circles) and  $^6\text{Li}$ (squares) vs the mass of the intermediate meson( $m_x$ ). The solid curves are the fits by a sum of polynomials minus a Gaussian.

## References

- [1] Bajukov J.D. *et al.*, Sov. Jad. Fis. 18(6) (1973) 1246.
- [2] Leksin G.A, Preprint ITEP 147, Moskow, (1976)
- [3] L.L.Frankfurt and M.I.Strikman, Phys.Rep. 76,214(1981);Phys.Rep. 160,235(1988)
- [4] Frankel S. *et al.*, Phys. Rev. C 24 (1981) 2684.
- [5] Frankel S. *et al.*, Phys. Rev. C 24 (1981) 2739.
- [6] Komarov V.I. *et al.*, Nucl. Phys. A 326 (1979) 297.
- [7] Baturin V.N. *et al.*, Preprint PNPI 1167 (1986)
- [8] Baturin V.N. *et al.*, Preprint PNPI 1747 (1991)
- [9] Baturin V.N. *et al.*, Preprint PNPI 1750 (1991)
- [10] Baturin V.N. *et al.*, Preprint PNPI 594 (1980)
- [11] V.N.Baturin *et al.*, Preprint PNPI 1154 (1986)
- [12] E.L.Berger *et al.*, Phys.Rev. D15 (1977) 206
- [13] DELPHI Coll., P.Abren *et al.*, Preprint CERN-PPE/94-02 (1994)
- [14] Dmitriev V., Sushkov O., Gaarde C., Nucl. Phys. A459 (1986) 503.
- [15] R.M.Sealock *et al.*, Phys.Rev.Lett. 62 (1989) 1350
- [16] O.V.Miklukho *et al.*, Preprint PNPI 2277 (1998).
- [17] A. Tang *et al.*, arXiv:nucl-ex/0206003.